Title
COMBUSTION-TURBULENCE INTERACTION IN THE TURBULENT BOUNDARY LAYER OVER A HOT SURFACE

Author
Ng, T.T.

Publication Date
1982

LBL-13893

Lawrence Berkeley Laboratory
UNIVERSITY OF CALIFORNIA

ENERGY & ENVIRONMENT DIVISION

To be presented at the 19th International Symposium on Combustion, Haifa, Israel, August 8-13, 1982

COMBUSTION-TURBULENCE INTERACTION IN THE TURBULENT BOUNDARY LAYER OVER A HOT SURFACE

T.T. Ng, R.K. Cheng, F. Robben, and L. Talbot

January 1982

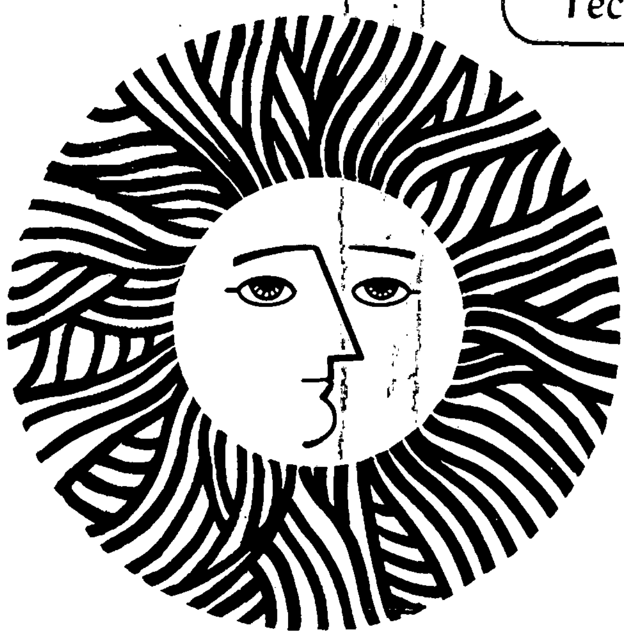

Prepared for the U.S. Department of Energy under Contract W-7405-ENG-48

DISCLAIMER

Combustion-Turbulence Interaction in the Turbulent Boundary Layer Over a Hot Surface

T.T. Ng, R.K. Cheng, F. Robben

Lawrence Berkeley Laboratory
University of California
Berkeley, California 94720

L. Talbot

Department of Mechanical Engineering
and Lawrence Berkeley Laboratory
University of California
Berkeley, California 94720

This work was supported by the Director, Office of Energy Research, Office of Basic Energy Sciences, Chemical Sciences Division of the U.S. Department of Energy under contract No. W-7405-ENG-48.

ABSTRACT

The turbulence-combustion interaction in a reacting turbulent boundary layer over a heated flat plate was studied. Ethylene/air mixture with equivalence ratio of 0.35 was used. The free stream velocity was 10.5 m/s and the wall temperature was $1250^{o}K$. Combustion structures visualization was provided by high-speed schlieren photographs. Fluid density statistics were deduced form Rayleigh scattering intensity measurements. A single-component laser Doppler velocimetry system was used to obtain mean and root-mean-square velocity distributions, the Reynolds stress, the streamwise and the cross-stream turbulent kinetic energy diffusion, and the production of turbulent kinetic energy by Reynolds stress. The combustion process was dominated by large-scale turbulent structures of the boundary layer. Combustion causes expansion of the boundary layer. No overall self-similarity is observed in either the velocity or the density profiles. Velocity fluctuations were increased in part of the boundary layer and the Reynolds stress was reduced. The turbulent kinetic energy diffusion pattern was changed significantly and a modification of the boundary layer assumption will be needed when dealing with this problem analytically.

I. Introduction

The initiation and sustentation of chemical reaction by a hot surface is a fundamental combustion problem pertinent to many practical situations such as the accidental ignition of a combustible mixture by a hot surface, the preignition of fuel-air mixture by hot-spots in an engine, and catalytic combustion over a hot surface. The initiation process and the sustentation process of combustion in boundary layers are different. Most experimental and theoretical studies to date had been focussed on the ignition aspect[1,2,3] and others on the physical influence of combustion on laminar boundary layers.[4,5] The main emphasis of the present study is on the sustentation of combustion and turbulence-combustion interactions in a reacting turbulent boundary layer.

Initiation of combustion in a boundary layer is characterized by the presence of cool flames as the first stage of a two-staged ignition process.[2] Toong[1] was one of the first to study, both theoretically and experimentally, the ignition in a laminar boundary layer. By assuming that ignition occurs when the fluid temperature gradient becomes zero near the surface, he found a good correlation between the surface temperature for incipient ignition and the free-stream velocity. This zero-gradient criterion has generally been adopted in later studies. Recently, Chen and Faeth[3] proposed an alternative wake ignition criterion which was shown to be more reliable in obtaining information on the ignition properties of heated surfaces.

The fluid mechanical influence of a premixed flame on a laminar boundary layer was examined theoretically by Trevino and Fernandez-Pello.[4] They found that curvature of the flame induces pressure gradients that affect the structure of the flow by perturbing the velocity field. In turbulent or wrinkled flame, where flame curvatures are prominent, the pressure distributions would be quite complex. Schefer et al.[5] studied combustion in a laminar boundary layer over a catalytic surface. They measured detailed velocity and temperature profiles and found different combustion characteristics dependent on the equivalence ratio and the surface temperature.

The objective of the present study is to examine the physical influence of combustion on the post-ignition region of a reacting turbulent boundary layer. The boundary layer over a flat surface was allowed to develope to the fully turbulent stage before ignition was induced by heating a section of the surface. This configuration is different from that of Cheng et al.[6] in which the velocity and the thermal boundary layer were developed almost simultaneously. Their results will be used later to compare with present findings.

High-speed schlieren photography was used for visualization of the combustion structures. Fluid density distributions were deduced from Rayleigh scattering intensity measurements; and a single-component laser Doppler velocimetry (LDV) system was used to obtain mean and root-mean-square (rms) velocity distributions, the Reynolds stress, the streamwise and the cross-stream turbulent kinetic energy diffusion, and the production of turbulent kinetic energy by Reynolds stress. The data presented in this report will mainly be the time-averaged statistical quantities relevant to momentum and turbulent kinetic energy transport.

II. Experimental Setup

Figure 1 shows a schematic of the experimental setup. The combustion flow was produced by a low-speed wind tunnel with a 10 cm square outlet. The wind tunnel was mounted on a three-dimensional traversing mechanism driven by a computer controlled stepping motor system to enable rapid scanning of the boundary layer by various diagnostic techniques. The boundary layer flow was developed over a 50 cm long, enclosed channel followed by a 25 cm long, opened heating section. The floor of the chanel was made up of two equal length segments: a sand-rough plate to accelerate the transition to turbulence, followed by a water-cooled plate to provide a stepwise temperature rise at the junction with the heating section. The heating section consists of nine 2.5 cm wide, 0.127 mm thick Kanthal A-1 alloy heating strips stretched by tension springs across evenly spaced recesses machined on a ceramic block to produce a flush surface. Each strip was electrically heated individually to give an fairly uniform wall temperature.

The wall temperature was measured by a disappearing filament optical pyrometer compensated for surface emissivity. A Spectra Physics model 164 4-Watt argon ion laser was used as the light source with the 488 nm line for the schlieren system and Rayleigh scattering intensity measurements, and the 514.5 nm line for the LDV system.

The schlieren setup consisted of an 18 mm focal length lens and a 1.0 m focal length, 75 mm diameter lens to collimate the laser light over the test section, and a second 1.0 m focal length, 75 mm diameter lens to focus the image of the test section onto a Fastax WF-17 16 mm high-speed movie camera. The maximum speed of the movie was about 3000 frames/sec. A standard knife edge was used as the schlieren stop.

The basic operating principle of the Rayleigh scattering system are described in several references.[7,8,9] Our system incorporated an 18 mm focal length lens and an 120 mm focal lens to focus the laser beam to a waist diameter of about 100 m. The scattered light from a 1 mm long beam section centered about the beam waist was collected at 90^{o} to the light path by a lens and photomultiplier assembly. The photomultiplier signal was amplified and recorded by the computer based data acquisition and control system described by Bill et al.[9]

The LDV setup used was a dual-beam differential system with the collection optics in the forward scattering direction. A TSI 1990 frequency counter was used to process the photomultiplier signal, and the counter output was recorded by the computer data acquisition system.

The procedure to obtain the mean velocity components, the rms velocity fluctuations, the Reynolds stress ($\overline{u'v'}$), and some higher-order correlations (e.g. $\overline{u'v'^2}$ and $\overline{v'u'^2}$) from single component LDV measurements are described elsewhere.[10]

The streamwise direction was denoted as x and the normal direction as y. The center of the leading edge of the heating section was designated as the origin. The counter and the Rayleigh scattering intensity output were recorded at a rate of 2500 samples/sec by the computer and 8192 samples were taken at each location.

III. Results and Discussions

Measurements were made for three different turbulent boundary layer flows: (1) isothermal, (2) stepwise heated wall, and (3) heated wall with combustion, all with free-stream velocity ($\bar{u}_o$) of 10.7 m/s and wall temperature (T_w) of 1250°K, measured by the optical pyrometer, for cases 2 and 3. The Rayleigh scattering data indicated a lower wall temperature; however, this discrepancy is not critical since a precise knowledge of the wall temperature is not essential to the overall goal of our experiment. For the reacting flow, an ethylene/air mixture with equivalent ratio of 0.35 was used. The results of the isothermal and the combustion flow will be compared and discussed in this report, and the results of the heated wall flow will appear in a subsequent paper.

The two-dimensionality of the flow was checked by inspecting velocity profiles in the horizontal cross-stream direction. At x = 150 mm, the flow remains fairly uniform at $\pm$ 25 mm from the center. To reduce the induction time for ignition, the first strip of the heating section was overheated by about $100^{o}K$.

Data were taken at predetermined y-positions at five streamwise stations (Table I). Measurements in the reacting flow were made after a "warm-up" period of about one hour to allow the heated surface to reach a steady state. The power supplied to the heating strips was reajusted to give a uniform wall temperature. Unfortunately, expansion of the strips caused some small unevenness on the surface which reflected stray light into the Rayleigh scattering collecting optics for measurements close to the surface. Hence, appropriate axial locations for Rayleigh scattering measurements were chosen to minimize this problem. Consequently, the station locations for the isothermal and the reacting boundary layer are slightly different.

The LDV data validation rate ranges from 12000 /sec in the free-stream to about 6000 /sec near the surface for the isothermal flow. For the combustion flow, the data rate near the surface was reduced to about 3000 /sec.

Schlieren photographs

Schlieren records of the reacting boundary layer are shown in fig. 2. Near the leading edge, as shown on the series on the left, the reaction zone is narrow and confined to regions near the surface. Surface heating and reaction precede the formation of detached flame structures (marked by the arrows). Blue luminosity typically associated with the cool flame can be seen by naked eyes near the leading edge. Farther downstream, the reaction zone consists of individual flame structures extend across the boundary layer as shown in the series on the right of fig. 2. These elongated structures are oriented at about 30^{o} to the surface and appear to be similar in structure. These flame characteristics are different from those described by Cheng et al.[6] where combustion seemed to occur in a continuous flame. In their experiment, the velocity and thermal boundary layer were developed almost simultaneously. Ignition therefore occurred in the laminar stage of the boundary layer. Due to the relatively low Reynolds number of their flow and the increase in viscosity in the hot wall region, a fully turbulent boundary layer was never attained.

In the present experiment, the boundary layer was fully turbulent when ignition was induced. If we interpret the discrete flame structures with reference to the cyclic development of large scale turbulent structures in a boundary layer as described by Kline et al.[11], Corino and Brodkey,[12] and Kim et al.,[13], the turbulent structures become the governing mechanism in sustaining the combustion process. The cyclic event of the reacting boundary layer can possibly be described as follows: i) combustible mixture is ignited by the hot surface and carried upwards by the "bursting" process; ii) fluid mixing and combustion continue to occur as the hot product is moving away from the surface and was convected downstream; iii) the "in-rushing" motion entrains fresh combustible mixture from the free-stream to the hot surface; iv) ignition occurs at the surface to complete the cycle.

Statistical Results

The development of the mean streamwise velocity profiles, $\overline{u}$, of the isothermal and the combusting flow are compared in fig. 3. No local streamwise acceleration due to fluid expansion was observed. Rather, the mean velocity of the reaction zone is slightly lower than at the same relative position in the isothermal boundary layer. The cross-stream velocity ($\bar{v}$), shown in fig. 4, is increased significantly, indicating a large streamline deflection away from the surface.

The boundary layer thickness, δ, the displacement thickness, δ_1, the momentum thickness, δ_2, and the thermal boundary layer thickness, δ_T, are listed in Table I. δ is defined at 99.5% of the free-stream velocity, u_o. δ_T is defined at 0.995 ($\rho_o - \bar{\rho}_b$), where ρ_o is the free-stream density and $\bar{\rho}_b$ the minimum density. For our experiment, the value of $\bar{\rho}_b / \rho_o$ derived from the Rayleigh scattering measurements was about 0.225. δ_1 and δ_2 are defined by[14]

$$\delta_1 = \int_0^\infty \left(1 - \frac{\bar{\rho}\bar{u}}{\rho_o \bar{u}_o} \right) dy \tag{1}$$

$$\delta_2 = \int_0^\infty \frac{\bar{\rho}\bar{u}}{\rho_o \bar{u}_o} \left(1 - \frac{\bar{u}}{\bar{u}_o} \right) dy \tag{2}$$

The Reynolds number based on the displacement thickness at $x = 0$ is about 900, which is higher than the generally cited critical value of about 600 for turbulent transition in a boundary layer. As shown by the increases in δ_1 and δ_2, combustion heat release expands the boundary layer. The derivatives of δ_2 suggest that the frition coefficient c_f is increased by combustion. This can be attributed to the increase in fluid viscosity. However, our data are too scattered for evaluating c_f accurately.

Mean density profiles are shown in fig. 5. At locations farther downstream, the profiles show a local minimum point away from the surface. The temperature associated with this minimum density is higher than the adiabatic flame temperature based on free-stream conditions.

This indicates that heat is transferred from the wall to the fluid near the leading edge of the heated wall region. The existence of a minimum density near the surface also indicates a reversed heat transfer from the reacting fluid to the wall. The shape of these profiles are similar to those observed in laminar boundary layer combustion[1,2,3].

No overall similarity is observed in either the velocity or the density profiles up to x = 100 mm. However, profiles obtained at stations farther downstream appear to be more self-similar.

Typical rms profiles of the isothermal boundary layer are compared with those of Corrsin and Kistler (Hinze[15]) for a rough surface. The agreement is fairly good. The free-stream turbulence is about 1%. Near the leading edge, rms velocity fluctuations in the wall region of the isothermal boundary layer are increased slightly. This indicates that additional turbulence is generated as the flow crosses from the smooth surface to the heating-section. Other fluctuation correlations in the wall region are consistently higher near the leading edge.

Rms velocity fluctuation profiles of the reacting boundary layer are shown in fig. 7. The presence of combustion in the boundary layer induces local peaks in both the $\hat{u}$ and $\hat{v}$ profiles. This is caused by the passage of flame structures across the stationary LDV probe. Near the leading edge where combustion is confined to a narrower region than farther downstream, the combustion induced peaks are also narrower and more distinct. These increases in $\hat{u}$ and $\hat{v}$ are quite different from the significant reduction in $\hat{u}$ due to combustion reported by Cheng et al.[6] This is because of the differences in the experimental configurations as mentioned earlier. In their experiment, the low initial Reynolds number and the increase in viscosity of the combustion products resulted in laminization of the boundary layer.

The density fluctuation profiles in fig. 8 show distinct peaks. The peaks are located close to the rms velocity peaks and the highest density gradient positions. Near the leading edge, the density fluctuations result mainly from ignition and combustion near the surface. Hence the peak $\hat{\rho}$ skews closer to the surface. At locations farther downstream, however, the density fluctuations are caused more by the passage of developed flame structures initiated at the hot surface upstream; hence the $\hat{\rho}$ profile is almost symmetrical. The $\hat{\rho}$ profile is narrower and has a high peak value near the leading edge, a result of the difference in the width of the reaction zones mentioned earlier.

The distribution of the non-dimensionalized Reynolds stress, $-\bar{\rho}\overline{u'v'}/\bar{\rho}_o\bar{u}_o^2$, is plotted in fig. 9. The Reynolds stress appears in the momentum balance equation of a variable density flow as

$$-\overline{\rho u'v'} = -(\bar{\rho}\overline{u'v'} + \overline{\rho' u'v'}) \qquad (3)$$

It is a common assumption that the contribution from the latter term is negligible, although there are few data to verify its validity in combustion flow. Nevertheless, measurements of triple correlations involving both the density and the velocity fluctuations are difficult; and our discussions on the Reynolds stress will be based on $-\bar{\rho}\overline{u'v'}$. The presence of combustion greatly reduces the value of $-\bar{\rho}\overline{u'v'}$. This reduction is due both to the decreases in density and in $\overline{u'v'}$. The decrease in $\overline{u'v'}$ indicates that the turbulent structures are now less organized.

Turbulent Kinetic Energy Diffusion and Production

The time-averaged differential equation governing the turbulent kinetic energy transport in combustion flows can be divided into four parts: (1) convection, (2) diffusion, (3) production, and (4) dissipation. Our discussions on the turbulent kinetic energy transport will be based on k_1 (= $u'^2 + v'^2$) instead of the full kinetic energy term (k) since the velocity component, w, in the z- direction was not measured. It is, however, reasonable to expect that the contributions of w′ will be similar to those of u′ and v′; thus the transport of k_1 will also be similar to that of k. Some of the transport quantities measured in our study are: the streamwise diffusion, $\overline{u'k_1}$; the cross-stream diffusion, $\overline{v'k_1}$; and the production due to Reynolds stress, $-\bar{\rho}\overline{u'v'}\partial\bar{u}/\partial y$.

The normalized $\overline{u'k_1}$ profiles are shown in fig. 10. The value of $\overline{u'k_1}$ in the isothermal boundary layer is negative, indicating that the fluid associated with negative u′ is more energetic. The very gradual change in the $\overline{u'k_1}$ profiles is consistent with the boundary layer assumption that streamwise diffusion for k_1 is not important. In the combustion case, the profiles are characterized by a second negative peak and a positive value of $\overline{u'k_1}$ close to the wall. The second peak seems to be closely associated with the development of the combustion structures. The original peak eventually disappears as the flow develops and the profiles resembles more those of the isothermal flow. The rapid changes in the $\overline{u'k_1}$ profile as contrast to the isothermal results indicate that significant streamwise kinetic energy diffusion is induced by combustion. Therefore, the boundary layer assumption has to be modified for the reacting boundary layer.

The $\overline{v'k_1}$ profiles are shown in fig. 11. The value of $\overline{v'k_1}$ is positive in the isothermal boundary layer, implying that the fluid associated with positive v′ (ejection burst) is more energetic. This form of $\overline{v'k_1}$ profile is typical of a turbulent boundary layer. Combustion heat release induces negative $\overline{v'k_1}$ near the surface. This indicates a reverse in the cross-stream turbulent kinetic energy diffusion direction. The negative value of $\overline{v'k_1}$ near the wall means that close to the surface, the fluid associated with negative v′ (inrushing fluid) is now more energetic.

The production of turbulent kinetic energy by Reynolds stress, $-\overline{\rho u'v'}\partial\overline{u}/\partial y$, was also evaluated and was found to be greatly reduced by combustion. The fact that kinetic energy does not decrease, but actually increases in some regions of the boundary layer either means that the dissipation rate has to decrease, which does not seem probable, or contributions from other production mechanisms have to be important. Further experiments are needed to establish whether these changes in the production and diffusion of the turbulent kinetic energy are caused by the density gradients and fluctuations, or by the complex pressure distributions induced by flame curvatures as mentioned by Trevino and Fernandez-Pello[5].

IV. Summary and Conclusions

The physical structure and statistical properties of a combusting turbulent boundary layer were studied by means of high-speed schlieren photography, Rayleigh scattering intensity measurements, and a single-component LDV system. Large-scale turbulence structures in the boundary layer dominate the combustion process with combustion occurring in individual flame structures rather than as a continuous flame sheet.

Combustion causes expansion of the boundary layer and large deflections of the mean streamlines away from the surface. The mean velocity profile is altered and no overall similarity is observed in either the velocity or the density profiles. The local wall friction coefficient is also increased due to the increase in fluid viscosity.

The presence of combustion increases velocity fluctuation levels in some parts of the boundary layer. Difference in the reaction zone width near the thermal leading edge and farther downstream result in different behaviors of the density and velocity fluctuations. The Reynolds stress is reduced by combustion; however, the result is not conclusive because of the absence of knowledge about the contribution from the $\overline{\rho' u' v'}$ term.

The kinetic energy production due to the Reynolds stress is reduced by combustion. This suggests that contributions from other production mechanisms may be important. Significant streamwise diffusion of turbulent kinetic energy is induced near the leading edge of the heating section, and a modification of the boundary layer assumption will be necessary when dealing with this problem analytically. The cross-stream diffusion pattern is also changed. The physical mechanisms that cause these changes in the turbulent kinetic energy transport are still unknown.

V. Nomenclature

c_f	friction coefficient
k_1	$u'^2 + v'^2$
Re_x	Reynolds number
$T(t)$	temperature
t	time
$u(t)$	streamwise velocity component
$v(t)$	cross-stream velocity
x	streamwise coordinate
y	cross-stream coordinate
δ	boundary layer thickness
δ_1	displacement thickness
δ_2	momentum thickness
δ_T	thermal boundary layer thickness
ρ	fluid density

Subscripts

o	reference condition
w	wall condition
b	minimum

Superscripts

$\bar{}$	average
$'$	fluctuation
$\hat{}$	root-meam-square

VI. Acknowledgements

This work was supported by the Director, Office of Energy Research, Office of Basic Energy Sciences, Chemical Sciences Division of the U.S. Department of Energy under contract No. W-7405-ENG-48.

VII. References

1. Toong, T. Y.: Sixth Symposium (Int'l) of the Combustion Institute, p.532, The Combustion Institute, 1957.

2. Cairnie, L. R., Harrison, A. J. and Summers, R.: First Specialists Meeting (Int'l) of the Combustion Institute, Vol. 2, p.366, The French Section of the Combustion Institute, 1981.

3. Chen, L. D. and Faeth, G. M.: First Specialists Meeting (Int'l) of the Combustion Institute, Vol. 2, p.395, The French Section of the Combustion Institute, 1981.

4. Trevino, C. and Fernandez-Pello, A. C.: First Specialists Meeting (Int'l) of the Combustion Institute, Vol. 1, p.249, The French Section of the Combustion Institute, 1981.

5. Schefer, R. W., Robben, F. and Cheng, R. K.: Combustion and Flame, Vol. 38, p.51, 1980.

6. Cheng, R. K., Bill, R. G. and Robben, F.: Eighteenth Symposium (Int'l) on Combustion, p.1021, The Combustion Institute, 1980.

7. Robben, F.: Comparison of Density and Temperature Measurement Using Raman Scattering and Rayleigh Scattering, Lawrence Berkeley Laboratory Report, LBL-3294, 1975.

8. Pitz, R. W., Cattolica, R., Robben, F. and Talbot, L.: Combustion and Flame, Vol. 27, p.313, 1976.

9. Bill, R. G., Jr., Namer, I., Talbot, L., Cheng, R. K. and Robben, F.: Combustion and Flame, Vol. 43, no. 3, p.229, 1981.

10. Ng, T. T.: Experimental Study of a Chemically Reacting Turbulent Boundary Layer, Ph.D. thesis, University of California, 1981.

11. Kline, S. J., Reynolds, W. C., Schraub, F. A. and Runstadler, P. W.: J. Fluid Mech., Vol. 30, Part 4, p.741, 1967.

12. Corino, E. R. and Brodkey, R. S.: J. Fluid Mech., Vol. 37, Part 1, p.1, 1969.

13. Kim, H. T., Kline, S. J. and Reynolds, W. C.: J. Fluid Mech., Vol. 50, Part 1, p.133, 1971.

14. White, F. M.: Viscous Fluid Flow, p.606, McGraw-Hill, 1974.

15. Hinze, J. O.: Turbulence, p.641, McGraw-Hill, 1975.

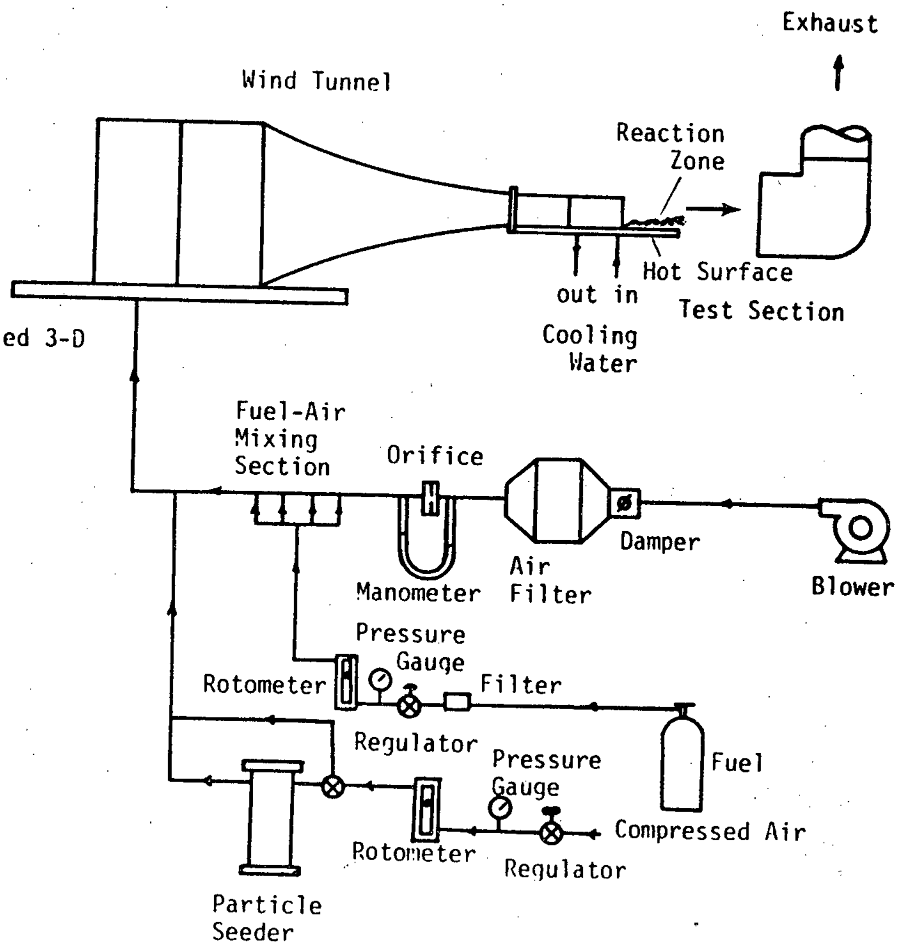

XBL 8112-12938

Fig. 1 Schematic of the experimental setup.

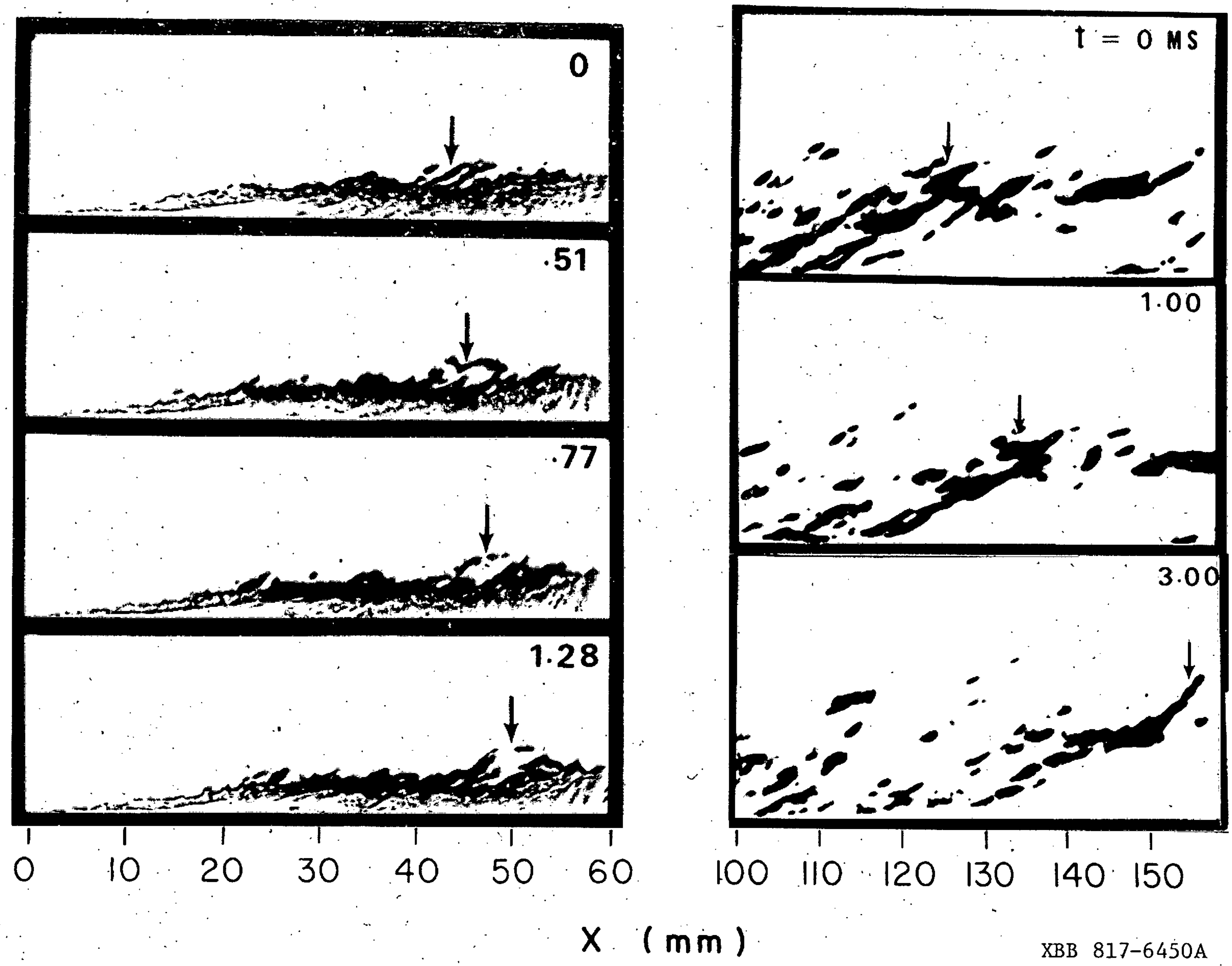

Fig. 2 Schlieren records of the reacting boundary layer.

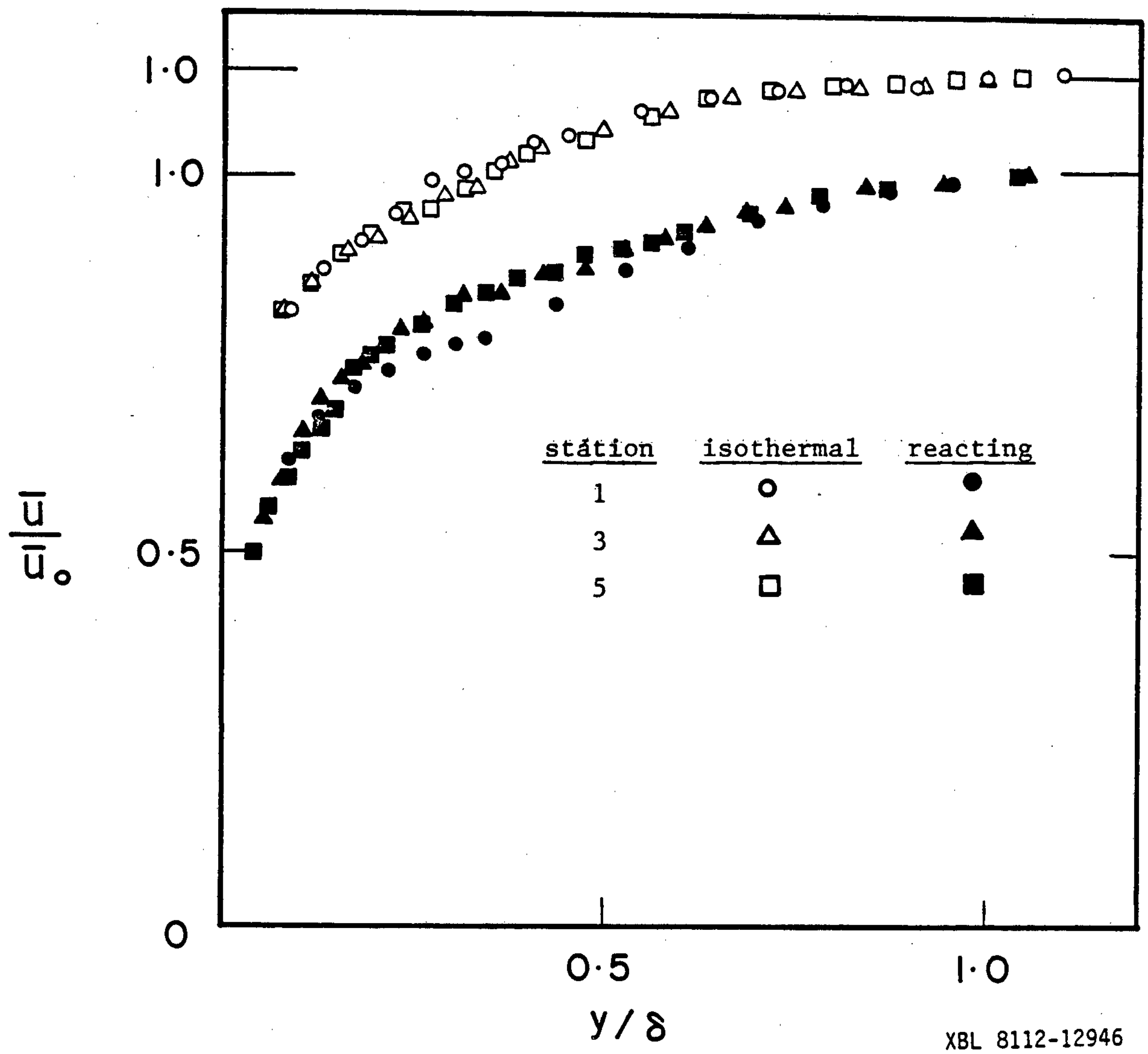

Fig. 3 Mean streamwise velocity profiles.

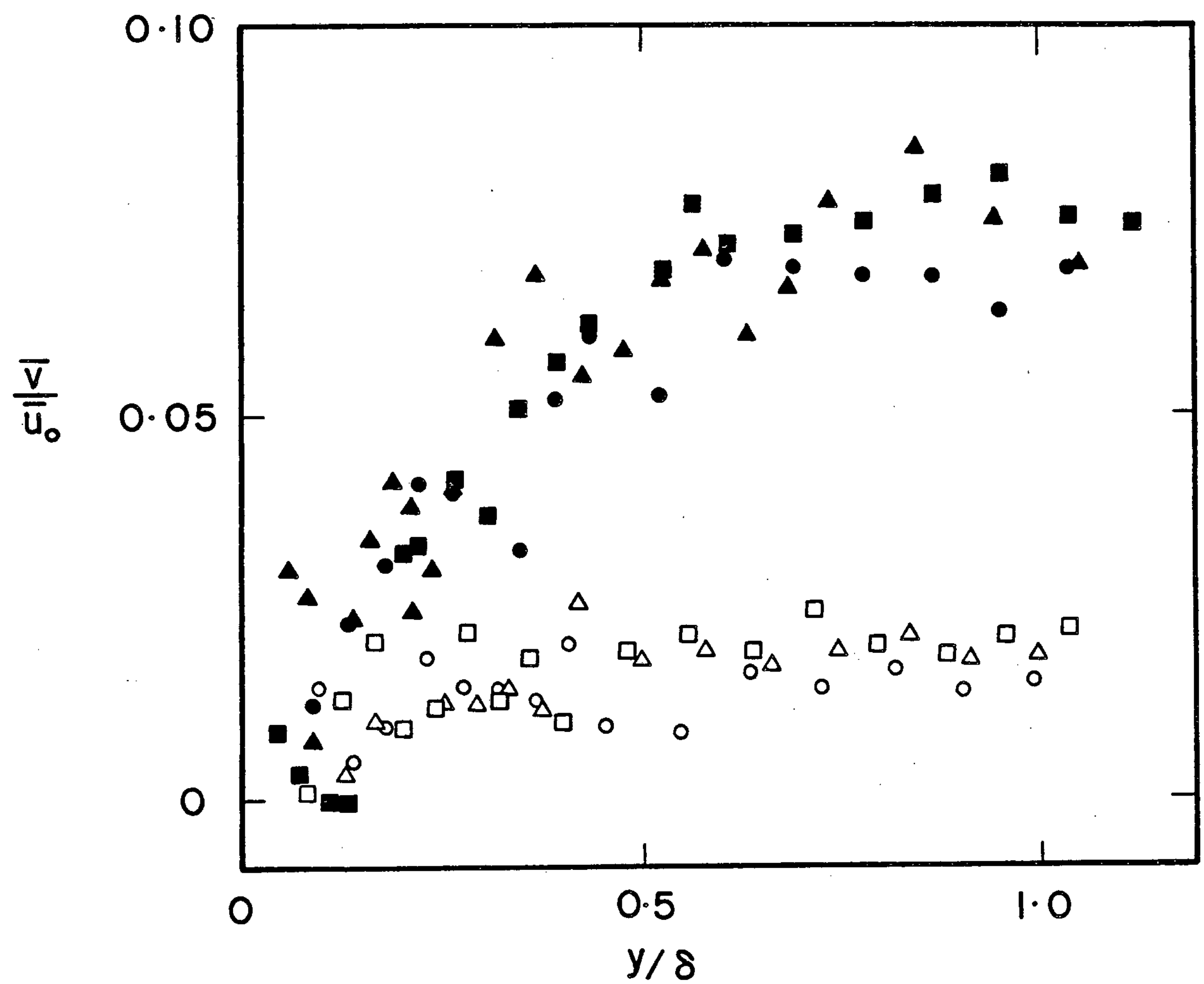

XBL 8112-12945

Fig. 4 Mean cross-stream velocity profiles.
(for symbols see fig. 3)

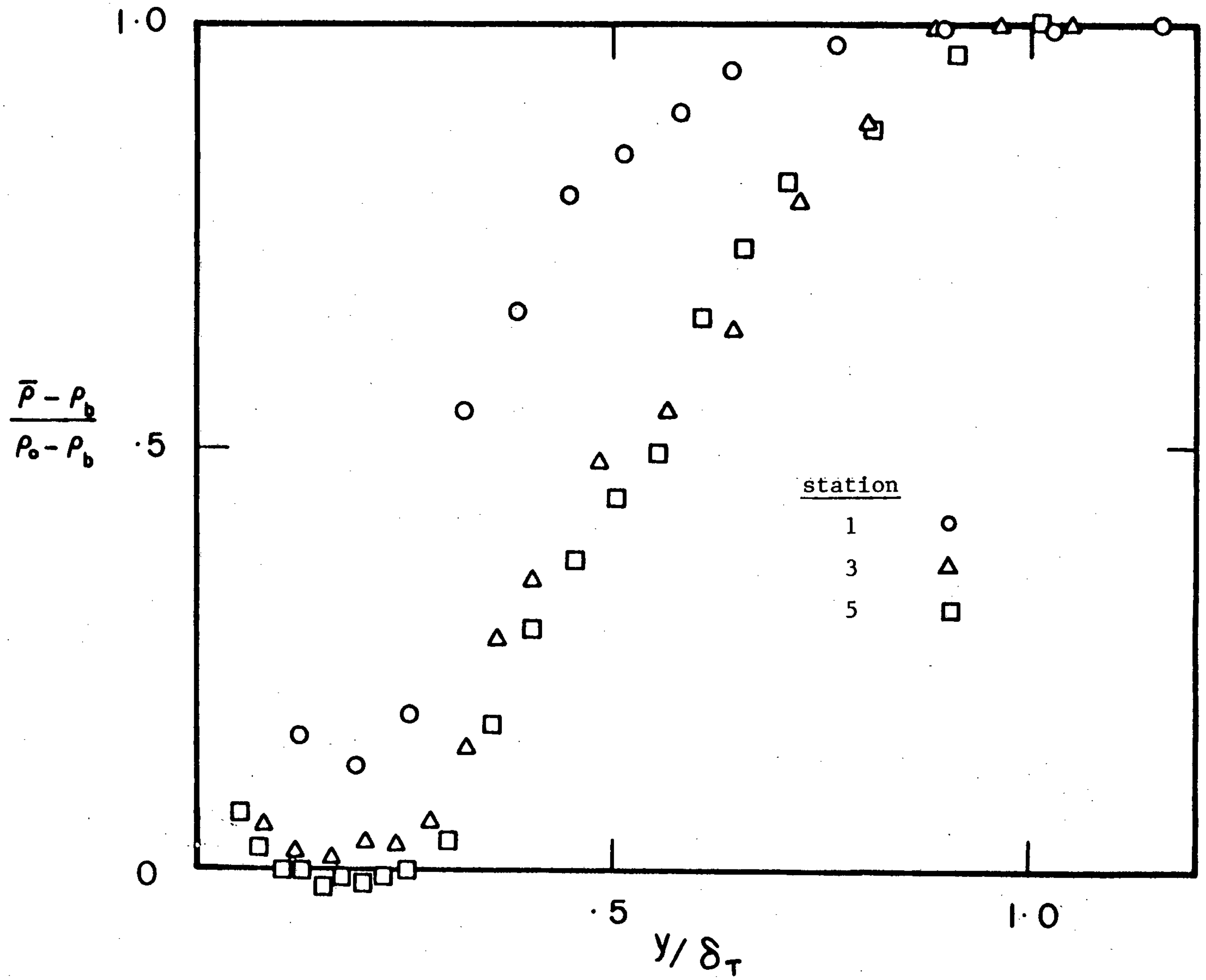

XBL 8112-12944

Fig. 5 Mean density profiles of the reacting boundary layer.

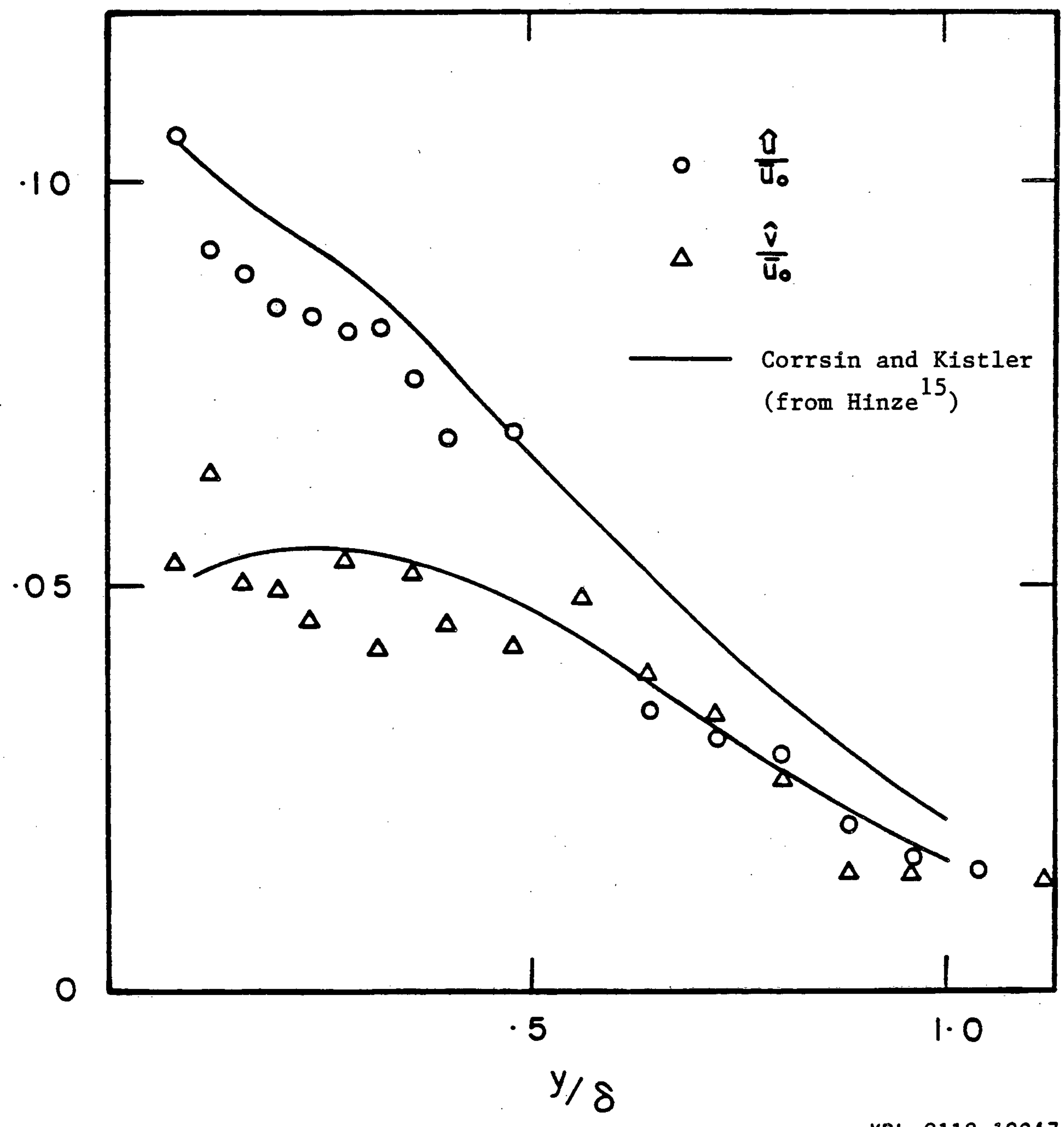

XBL 8112-12947

Fig. 6 Rms velocity fluctuation profiles of the isothermal boundary layer at station 5.

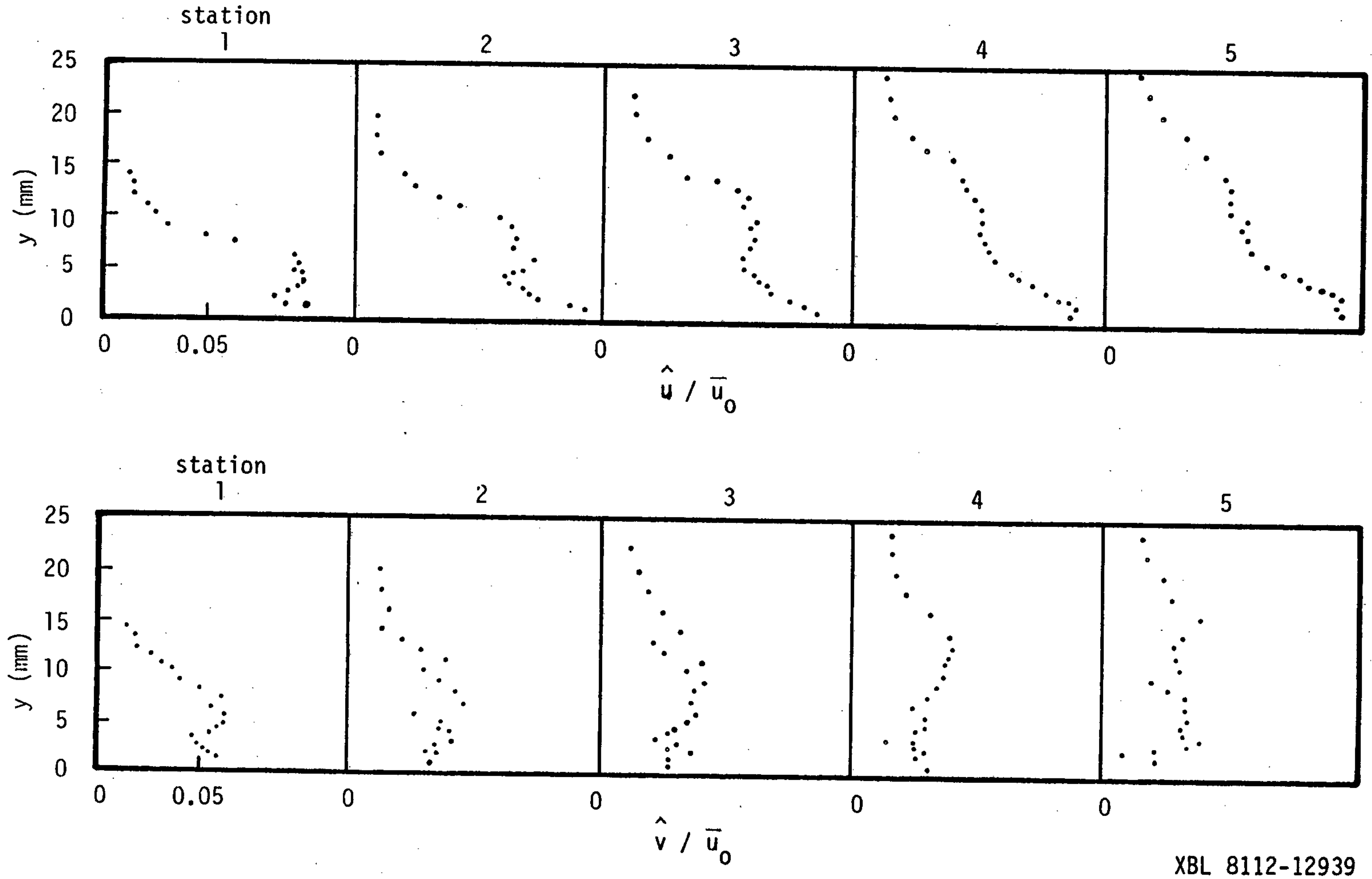

Fig. 7 Rms velocity fluctuation profiles of the reacting boundary layer at several axial stations.

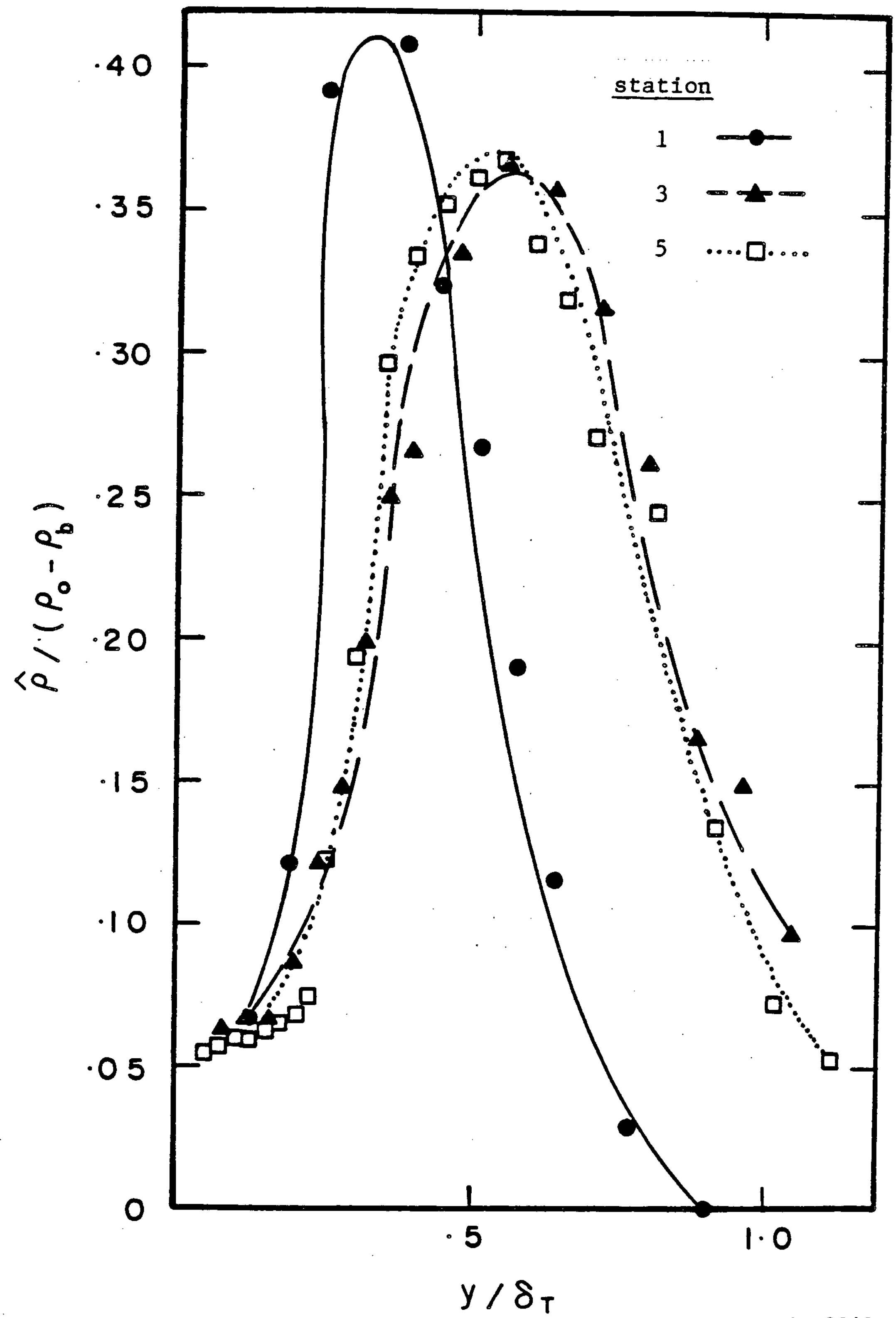

XBL 8112-12940

Fig. 8 Rms density fluctuation profiles of the reacting boundary layer.

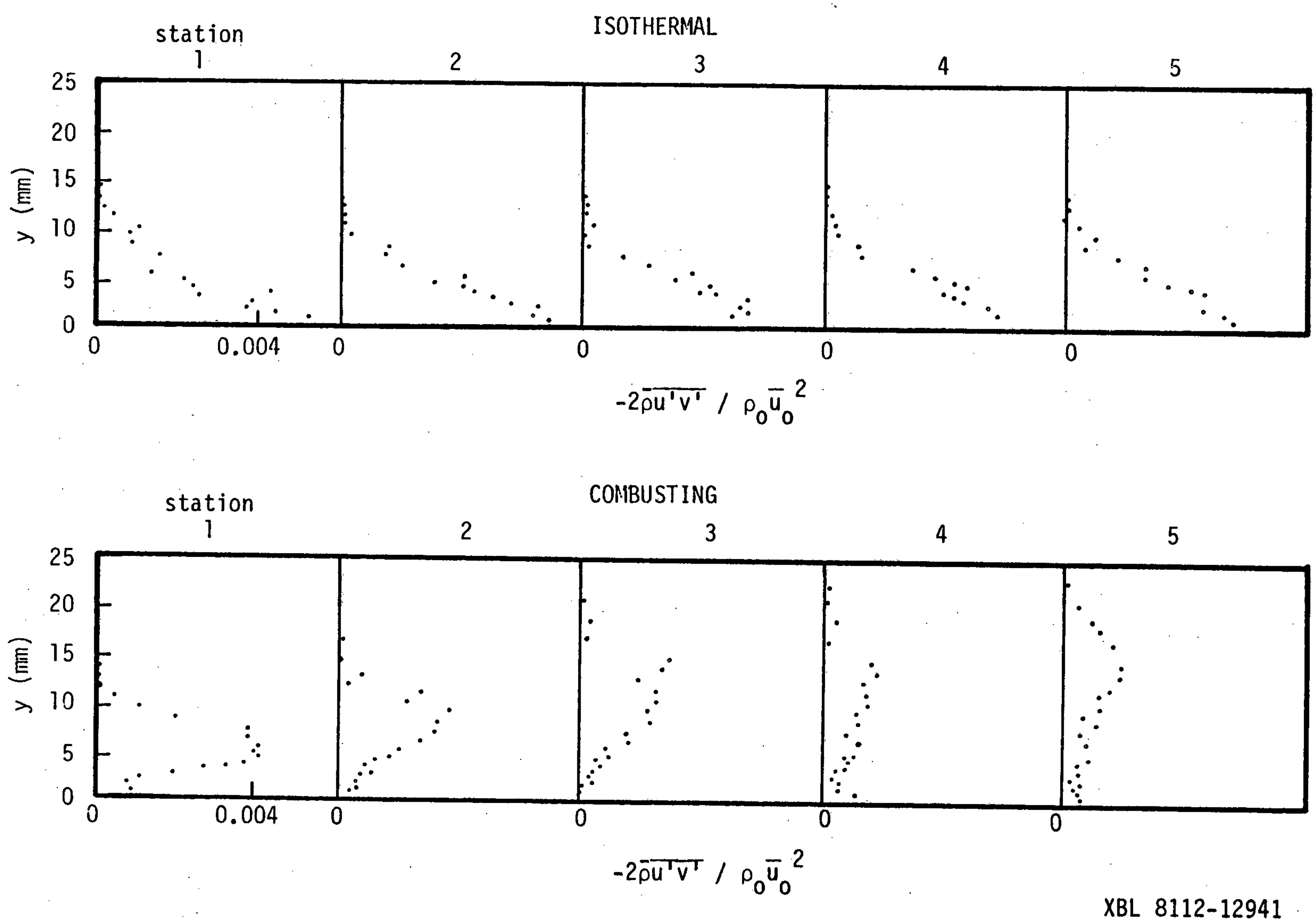

Fig. 9 Reynolds stress profiles of the isothermal and the reacting boundary layer at several axial stations.

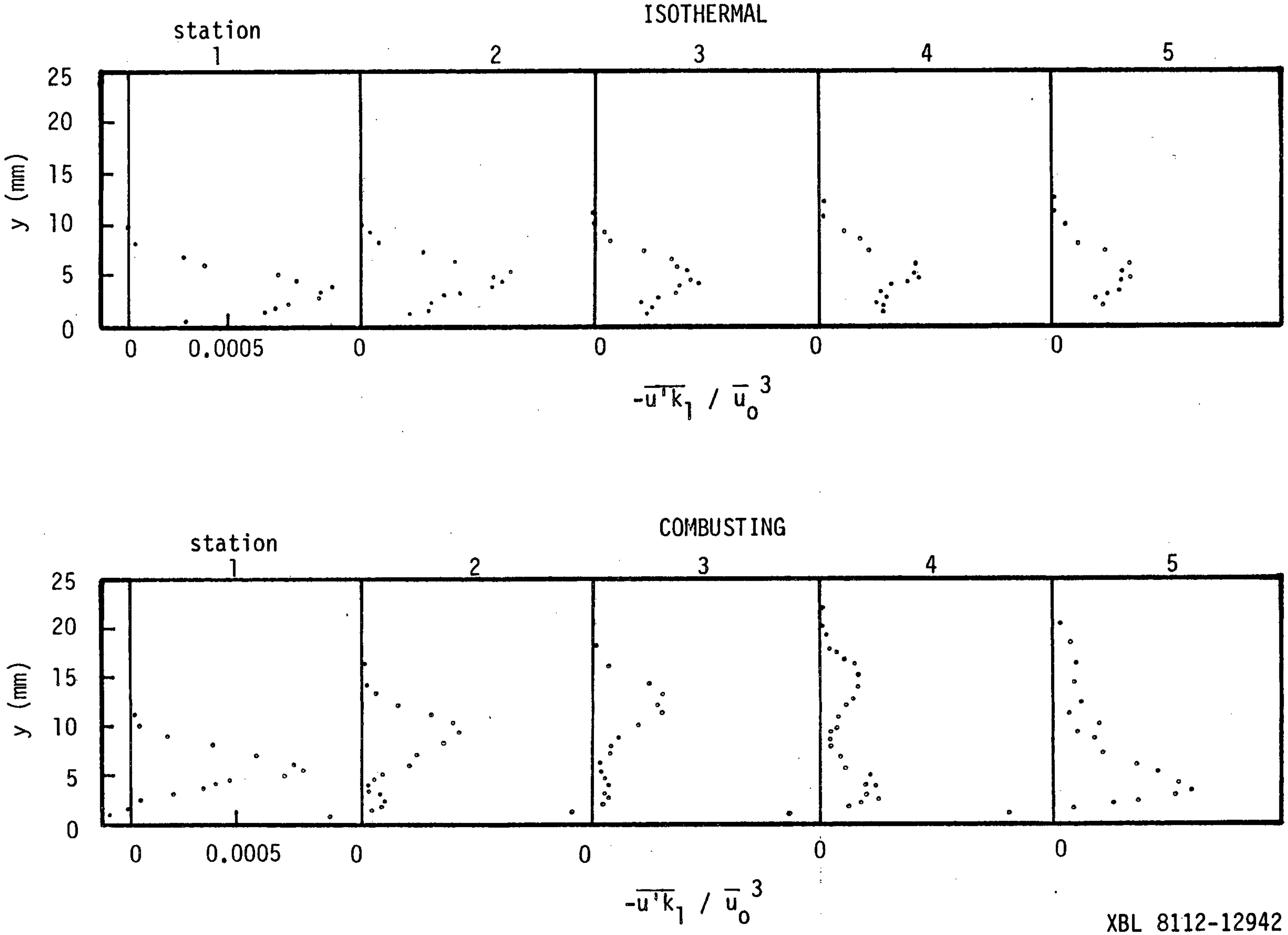

Fig. 10 Streamwise turbulent kinetic energy diffusion of the isothermal and the reacting boundary layer at several axial stations.

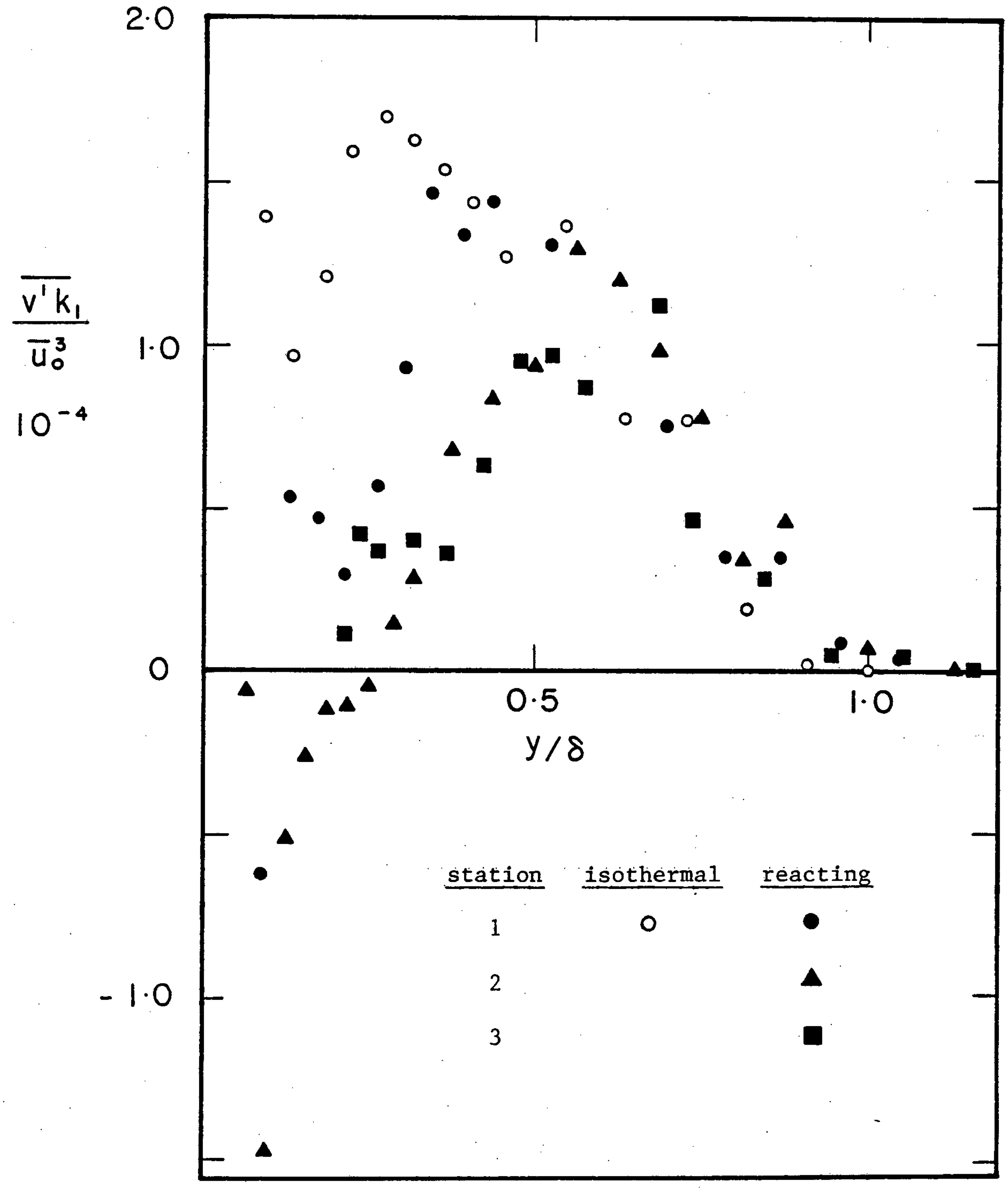

XBL 8112-12943

Fig. 11 Cross-stream turbulent kinetic energy diffusion of the isothermal and the reacting boundary layer at several axial stations.

ISOTHERMAL						COMBUSTING				
Station	x	δ	δ_1	δ_2		x	δ	δ_1	δ_2	δ_T
(mm)										
1	33	11.0	1.56	0.86		33	11.5	3.34	0.89	7.8
2	70	11.0	1.73	0.96		62	16.0	5.08	0.89	11.2
3	103	12.0	1.70	0.97		90	19.0	6.45	1.02	12.4
4	130	12.5	1.55	0.86		123	21.0	8.09	1.09	18.6
5	150	12.5	1.77	1.02		148	23.0	9.88	0.97	19.7

Table I Boundary layer thickness, displacement thickness, momentum thickness, and thermal boundary layer thickness.

TECHNICAL INFORMATION DEPARTMENT
LAWRENCE BERKELEY LABORATORY
UNIVERSITY OF CALIFORNIA
BERKELEY, CALIFORNIA 94720